# Optimal preparation of high-entropy boride-silicon carbide ceramics

**Yan Zhang**
Guangdong University of Technology
**Shi-Kuan Sun**
The University of Sheffield
**Wei-Ming Guo** ( guo1237@126.com )
**Liang Xu**
Guangdong University of Technology
**Wei Zhang**
Guangdong University of Technology
**Hua-Tay Lin**
Guangdong University of Technology

**Rapid Communication**

**Keywords:** High-entropy boride-silicon ceramics, Borothermal reduction, Boro/carbothermal reduction, Microstructure, Mechanical properties

**Posted Date:** August 7th, 2020

**DOI:** https://doi.org/10.21203/rs.3.rs-33290/v2



**Version of Record:** A version of this preprint was published at Journal of Advanced Ceramics on October 21st, 2020. See the published version at https://doi.org/10.1007/s40145-020-0418-1.

# Abstract

High-entropy boride-silicon carbide (HEB-SiC) ceramics were fabricated by using boride-based powders prepared from borothermal and boro/carbothermal reduction methods. The effects of processing routes (borothermal reduction and boro/carbothermal reduction) of HEB powders were examined. HEB-SiC ceramics with nearly relatively full density (>98%) were prepared by spark plasma sintering at 2000oC. It was demonstrated that the addition of SiC led to slightly coarsening of the microstructure. The HEB-SiC ceramics prepared from boro/carbothermal reduction powders showed the fine-grained microstructure and higher Vickers' hardness but lower fracture toughness values as compared with the same composition prepared from borothermal reduction powders. These results indicated that the selection of the powder processing method and the addition of SiC phase could contribute to the optimal preparation of high-entropy boride-based ceramics.


# 1. Introduction

In recent years, high-entropy ultra-high temperature boride (HEB) ceramics have been extensively studied by combining the concepts of ultra-high temperature boride ceramic (UHTC) and high-entropy materials [1–3]. HEB ceramics were found to exhibit high hardness and superior oxidation resistance [4–6]. Accordingly, HEB ceramics were considered to possess potential for the broad application [4]. On the other hand, HEB ceramics suffered from the difficulty in densification mainly due to the strong covalent-bonded nature and low diffusion rate during sintering process, as previously observed in traditional UHTC boride system (e.g. $ZrB_2$ and $HfB_2$) [4, 5, 7, 8]. Gild *et al.* [4] fabricated high-entropy boride ceramics by the combination of high-energy ball milling of the raw boride precursors and spark plasma sintering (SPS) at 2000 °C. The as-sintered materials exhibited relative higher hardness (21.0 ~ 22.5 GPa) and better oxidation resistance as compared to traditional boride ceramics. However, the relative density reported was reported to be only 92.4%. Our recent works reported that HEB ceramics could reach higher relative densities of 95.0 ~ 99.2% by sintering the HEB powder derived from borothermal reduction and 96.3 ~ 98.5% from boro/carbothermal reduction, respectively [9, 10]. It was shown that HEB material with nearly full densification (RD = 99.2%) and remarkable hardness (28.3 ± 1.6 GPa) could be achieved in the system of $(Hf_{0.2}Zr_{0.2}Ta_{0.2}Cr_{0.2}Ti_{0.2})B_2$ [9].

By reviewing the developmental progress of ultra-high temperature boride ceramics, SiC was added as the secondary phase into $ZrB_2$ and $HfB_2$ system with the purposes to reduce the sintering temperature, to suppress the abnormal grain growth, and to improve the mechanical properties and the oxidation resistance [11–13]. However, a few studies had been performed regarding the addition of SiC into HEB ceramics system. In a recent study, $B_4(HfMo_2TaTi)C$-$SiC_w$ showed an extremely high Vickers' hardness (35.4 GPa) and excellent oxidation resistance [14]. The introduction of SiC to HEB ceramic system was reported to improve the densification behaviour as well as mechanical properties [15]. $(Ti_{0.2}Zr_{0.2}Hf_{0.2}Nb_{0.2}Ta_{0.2})B_2$-SiC was fabricated with high density (> 97%) by SPS at 1900 °C, and the fracture toughness was increased by more than 30% [15]. Recently, Liu *et al.* reported the addition of 20 vol% SiC into $(Ti_{0.2}Zr_{0.2}Hf_{0.2}Nb_{0.2}Ta_{0.2})B_2$ high entropy ceramics prepared by hot pressing sintering at 1800 °C, improved the four-point flexural strength, fracture toughness, and hardness $Hv_{0.2}$ from 339 ± 17 MPa, 3.81 ± 0.40 MPa·$m^{1/2}$, and 23.7 ± 0.7 GPa to 447 ± 45 MPa, 4.85 ± 0.33 MPa·$m^{1/2}$, and 24.8 ± 1.2 GPa, respectively [16]. Nevertheless, more studies on HEB-SiC

ceramic system would be still required to understand the effects of the powder processing methods and the addition of SiC on the densification behaviour and mechanical properties of HEB-SiC ceramics.

In this work, the self-synthesised HEB powders were mixed with SiC particles and sintered by SPS. In particular, the processing methods were examined between the HEB powders prepared by borothermal reduction and boro/carbothermal reduction. The HEB ceramic systems, namely $(Hf_{0.2}Zr_{0.2}Mo_{0.2}Nb_{0.2}Ti_{0.2})B_2$ and $(Hf_{0.2}Mo_{0.2}Ta_{0.2}Nb_{0.2}Ti_{0.2})B_2$, were chosen in line with our previous studies [9, 10]. The influences of the powder-processing routes on the phase assemblage, microstructure, and mechanical properties of HEB-SiC ceramics were emphatically investigated in this study.

# 2. Experimental Procedure

Raw powders used in this study were $HfO_2$ (~ 0.3 μm, purity ≥ 99.95%, Beijing Founde Star Sci. & Tech. Co., Ltd, China), $ZrO_2$ (~ 0.6 μm, ≥ 99.8%, Changsha Xili Nanometer Lapping Tech. Co., Ltd, China), $Nb_2O_5$ (~ 2.0 μm, ≥ 99.95%, Beijing Founde Star Sci. & Tech. Co, Ltd, China), $TiO_2$ (~ 21 nm, ≥ 99.9%, Xuancheng Jingrui New Material Co., Ltd, China), $Ta_2O_5$ (~ 0.5 μm, ≥ 99.95%, Zhuzhou Cemented Carbide Group Co., Ltd, China), $MoO_3$ (~ 1.0 μm, ≥ 99.9%, Shanghai Naiou Nano Tech. Co., Ltd, China), boron (~ 1 μm, > 95.60%, Dandong Chemical Engineering Institute Co., Ltd, Dandong China), $B_4C$ (~ 1.5 μm, ≥ 99.9%, Mudanjiang Diamond Boron Carbide Co. Ltd, China), and graphite (~ 2.0 μm, ≥ 99.9%, Shanghai Colloid Chemical Co., Ltd, China). The appropriate amount of the raw powders was batched and mixed by roller milling in ethanol for 24 hours to target the fabrication of $(Hf_{0.2}Zr_{0.2}Mo_{0.2}Nb_{0.2}Ti_{0.2})B_2$ and $(Hf_{0.2}Mo_{0.2}Ta_{0.2}Nb_{0.2}Ti_{0.2})B_2$. Processes of borothermal reduction (from oxide and boron) and boro/carbothermal reduction (from oxide, boron carbide and graphite) were separately employed to prepare HEB powders by heat-treating the pre-mixed powders at 1600$^{o}$C for 1 h under vacuum. The purity of $(Hf_{0.2}Zr_{0.2}Mo_{0.2}Nb_{0.2}Ti_{0.2})B_2$ and $(Hf_{0.2}Mo_{0.2}Ta_{0.2}Nb_{0.2}Ti_{0.2})B_2$ powders was 86.8 wt% and 97.3 wt% through borothermal reduction [9]; 94.0 wt% and 93.0 wt% through boro/carbothermal reduction, respectively [10]. More details on the purity and particle size on HEB powders synthesized could be found in Refs. [9] and [10]. 20 vol.% SiC (~ 0.3 μm, ≥ 99.9%, Shanghai Xiangtian New-Materials Co., Ltd, China) were mixed with the as-obtained HEB powders and sintered by spark plasma sintering (H-HPD 10-FL, FCT System Gmbh, Germany) at 2000$^{o}$C in argon atmosphere with a ramping rate of 150$^{o}$C/min and the uniaxial pressure of 30 MPa (the same process parameters as the HEB ceramics without SiC additive [9, 10]). $(Hf_{0.2}Zr_{0.2}Mo_{0.2}Nb_{0.2}Ti_{0.2})B_2$-SiC and $(Hf_{0.2}Mo_{0.2}Ta_{0.2}Nb_{0.2}Ti_{0.2})B_2$-SiC derived from borothermal reduction were labelled as HSBR-1 and HSBR-2, respectively. Similarly, the HEB samples from boro/carbothermal reduction were designated as HSBCR-1 and HSBCR-2.

The density of the HEB-SiC specimens was measured according to Archimedes' principle. The theoretical density of the HEB ceramics was calculated by rule of mixture. The purity of the SPSed samples was examined by powder X-ray diffraction (XRD; D8, Bruker Co., Germany) on powder samples after crushing the sintered HEB-SiC specimens. On the other hand, the microstructure was examined by scanning electron microscopy (SEM; Nova NanoSEM430, FEI, Netherlands) equipped with energy dispersive X-ray spectra analysis (EDS; Quantax 200, Bruker Co.). The average grain size of HEB phase in the SPSed HEB-SiC samples was estimated from SEM images after etching. Vickers' hardness ($Hv_{0.2}$) of the ceramics was measured using

a Vickers' Hardness Tester (HVS-30Z, Shanghai Taiming Optical Instrument Co., Ltd, China) with the load of 200 gf for 15 seconds, and at least 10 indentation points per sample were tested. HEB-SiC ceramics were measured by indentation method with the load of 10 kgf for 10 seconds (> 10 indentation points per sample) and toughness value was calculated accordingly [17].

# 3. Results And Discussion

The relative density (RD) of the specimen was measured to be 100% and 99.1% for HSBR-1 and HSBR-2, respectively, indicative of nearly full densification, as listed in Table 1. In contrast with HEB ceramics without SiC phase (97.7% and 95.0% in the same composition without SiC in Ref. [9], 98.1% and 98.5% in Ref. [10]), the densification of HEB ceramic material was apparently improved by the introduction of SiC. Close values of RD were determined for the HSBCR series samples from boro/carbothermal reduction, suggested that there was no obvious difference regarding the densification response between processing methods of borothermal reduction and boro/carbothermal reduction.

Powder XRD patterns of the HEB-SiC ceramics after SPS at 2000$^{o}$C were provided in Fig. 1A. Characteristic peaks of high-entropy boride phase were identified (space group of *P6/mmm*). In comparison with $ZrB_2$ and $HfB_2$, the peaks of HEB phase shifted to the higher $2\theta$ range, indicative of the formation of the smaller crystal cell. Meanwhile, the reflections of α-SiC were detected at $2\theta = 34.1^{o}$ and $35.6^{o}$ (as shown in Fig. 1B) and the peak intensities were weaker than those of HEB ceramic phase. In addition, the contamination of the oxide impurity ($HfO_2$) was observed in the HEB-SiC ceramics, similar to our previously reported studies [9, 10]. It should be noted that the intensity of $HfO_2$ peaks in the product prepared by boro/carbothermal reduction was weaker than those by borothermal reduction. This was likely due to the remaining carbon impurities present after boro/carbothermal reduction, which anticipated to react with the oxide impurity during the sintering process, and therefore facilitated the formation of HEB phase. The lattice parameters calculated by Rietveld refinement were also listed in Table 1. No obvious variations in lattice parameters were observed among all HEB phases prepared from borothermal reduction and boro/carbothermal reduction method.

Table 1
Summary of the results on high-entropy boride-SiC ceramics in comparison with the reported results [4,9,10].

| Composition | a (Å) | c (Å) | HE phase grain size (μm) | Relative density (%) | Hv(GPa) | $K_{IC}$ (MPa·$m^{1/2}$) |
|---|---|---|---|---|---|---|
| HSBR-1: $(Hf_{0.2}Zr_{0.2}Mo_{0.2}Nb_{0.2}Ti_{0.2})B_2$-20 vol% SiC | 3.0981 | 3.3645 | 3.99 ± 0.73 | 100 | 25.8 ± 1.2 | 4.53 ± 0.66 |
| HSBR-2: $(Hf_{0.2}Mo_{0.2}Ta_{0.2}Nb_{0.2}Ti_{0.2})B_2$-20 vol% SiC | 3.0812 | 3.3059 | 4.18 ± 0.96 | 99.1 | 26.2 ± 1.8 | 4.41 ± 0.21 |
| HSBCR-1: $(Hf_{0.2}Zr_{0.2}Mo_{0.2}Nb_{0.2}Ti_{0.2})B_2$-20 vol% SiC | 3.0980 | 3.3696 | 3.00 ± 0.57 | 98.6 | 29.0 ± 1.3 | 3.80 ± 0.33 |
| HSBCR-2: $(Hf_{0.2}Mo_{0.2}Ta_{0.2}Nb_{0.2}Ti_{0.2})B_2$-20 vol% SiC | 3.0875 | 3.3058 | 3.75 ± 0.89 | 100 | 28.1 ± 0.9 | 4.25 ± 0.37 |
| $(Hf_{0.2}Zr_{0.2}Mo_{0.2}Nb_{0.2}Ti_{0.2})B_2$[9] | 3.0934 | 3.3526 | * | 97.7 | 26.3 ± 0.7 | * |
| $(Hf_{0.2}Mo_{0.2}Ta_{0.2}Nb_{0.2}Ti_{0.2})B_2$[9] | 3.0820 | 3.3065 | * | 95.0 | 25.9 ± 1.1 | * |
| $(Hf_{0.2}Zr_{0.2}Mo_{0.2}Nb_{0.2}Ti_{0.2})B_2$[10] | 3.0945 | 3.3592 | 1.45 | 98.1 | 26.3 ± 1.8 | * |
| $(Hf_{0.2}Mo_{0.2}Ta_{0.2}Nb_{0.2}Ti_{0.2})B_2$[10] | 3.0821 | 3.2810 | 1.86 | 98.5 | 27.0 ± 0.4 | * |
| $(Hf_{0.2}Zr_{0.2}Mo_{0.2}Nb_{0.2}Ti_{0.2})B_2$ [4] | 3.092 | 3.345 | * | 92.3 | 21.9 ± 1.7 | * |
| $(Hf_{0.2}Mo_{0.2}Ta_{0.2}Nb_{0.2}Ti_{0.2})B_2$ [4] | 3.082 | 3.279 | * | 92.2 | 22.5 ± 1.7 | * |

EDS element mapping was adopted to identify the impurity in HEB-SiC ceramics and shown in Fig. 2. The grey phase observed as the matric was high-entropy boride, and the dark-grey phase was SiC. The white phase was considered as the oxide impurity, consistent with the XRD result. Result of EDS mapping showed that the distribution of each element for each HEB-SiC ceramic was uniform. SiC phase exhibited homogeneous distribution in the HEB phase matrix with no agglomeration or no solid solution with other elements from HEB.

The polished surface of the HEB-SiC ceramic after etching was shown in Fig. 3. Observations showed that SiC mainly distributed in triple grain junctions. The average grain size of HEB phase in the composition was measured to be 3.99 ± 0.73 μm in HSBR-1, 4.18 ± 0.96 μm in HSBR-2, 3.00 ± 0.57 μm in HSBCR-1, and 3.75 ± 0.89 μm in HSBCR-2, respectively. In our previous study [10], HEB ceramics without SiC prepared from

borothermal reduction owned a relatively fine microstructure and the average grain size was 1 ~ 2 μm (Table 1). The enhanced grain growth in the current HEB-SiC ceramics was apparent as compared with the HEB ceramics without SiC under the same sintering condition. This was upexpected as SiC was typically considered to refine the microstructure of simple diboride ceramics (e.g. $ZrB_2$), by means of the pinning effects. Whereas, the opposite phenomenon was observed for both HEB-SiC products prepared by two powder processing route. This might suggest the introduction of SiC into the HEB ceramics may accompany with liquid phase sintering, as oxygen impurity from SiC (in format of $SiO_2$) may form eutectic phase and further enhance the grain growth of the HEB phase. Further experiments are under investigation to explain the mechanism and this work may provide some guidance for microstructure tuning of the HEB materials.

The average particle size of the starting HEB compounds from either borothermal reduction and boro/carbothermal reduction are measured to be in the range of 0.3 ~ 0.6 μm [9, 10]. The microstructure of the HEB-SiC ceramics derived from borothermal reduction was expected to be comparable than that from boro/carbothermal reduction. However, from the microstructure analysis, it should be noted that a relatively fine grain size of HEB phase was observed in the HSBCR-1 and HSBCR-2 samples from boro/carbothermal reduction. This indicated that the processing routes of HEB powder would affect the microstructure of the final HEB-SiC ceramics. This difference could be attributed to the fact that the presence of oxygen impurity or liquid phase would promote the coarsening of boride grains, however, that carbon residues present during boro/carbothermal reduction could facilitate the removal of oxygen impurity by carbothermal reduction and hence the grain growth of HEB phase was possibly suppressed during sintering at high temperature [12, 13]. In addition, finer SiC particles were also observed in the samples prepared by boro/carbothermal reduction, which could be explained by the grain size of HEB phase in HSBCR-1 and HSBCR-2 was smaller than that in the HSBR-1 and HSBR-2, which isolated SiC particles and suppressed the mass transfer and growth of the SiC grains by providing a longer diffusion path.

The fracture surfaces of HEB-SiC ceramics were shown in Fig. 4. Microstructure observations exhibited few pores and dense morphology in all compositions. The grey phase observed was high-entropy boride and the dark-grey phase was SiC particles. All the sintered specimens showed a transgranular fracture on the HEB phase. However, intergranular fracture behaviour on SiC grain was evident. A clear grain-pull-out and intergranular fracture of some SiC grains were observed in Fig. 4a and b, which was absent on the microstructures derived from boro/carbothermal reduction (Fig. 4c and d). The reason was likely caused by removal of oxygen impurity in boro/carbothermal reduction, as a consequence, the grain boundary was purified and the bonding between grains was strong, leading to the transgranular fracture.

Measurements of Vickers' hardness and fracture toughness of the HEB-SiC ceramics were provided in Table 1. The hardness values were 25.8 ± 1.2 GPa and 26.2 ± 1.8 GPa in HSBR-1 and HSBR-2, respectively. It was noteworthy that Vickers' hardness of HEB-SiC derived from boro/carbothermal reduction showed the high values of 29.0 ± 1.3 GPa in HSBCR-1 and 28.1 ± 0.9 GPa in HSBCR-2. This could be attributed to the refined microstructure of HEB-SiC derived from boro/carbothermal reduction. The toughness values were 4.53 ± 0.66 $MPa{\cdot}m^{1/2}$ and 4.41 ± 0.21 $MPa{\cdot}m^{1/2}$ in HSBR-1 and HSBR-2, respectively. The toughness value 3.80 ± 0.33 $MPa{\cdot}m^{1/2}$ and 4.25 ± 0.37 $MPa{\cdot}m^{1/2}$ in HSBCR-1 and HSBCR-2, respectively. The HEB ceramics from

borothermal reduction showed slightly higher toughness values, due to grain pull-out effect of some SiC grains (see Fig. 4), which was assumed to deflect the crack propagation.

It could be concluded that boro/carbothermal reduction route would not only refine the microstructure but also enhance the hardness of the final specimens. Meanwhile, the addition of SiC unexpectedly promoted the grain growth of high entropy boride phase in comparison with HEB ceramics without SiC. It was showed that the fracture toughness of HEB-SiC from borothermal reduction slightly increased with SiC addition. These findings provided a better understanding of processing route, the densification, and mechanical performance of high-entropy boride-silicon carbide ceramics. The results may inspire the further optimisation of both microstructure and mechanical properties of high-entropy boride materials for potential applications.

# 4. Conclusion

The processing routes of high-entropy boride powder via borothermal and boro/carbothermal reduction were examined and compared on $(Hf_{0.2}Zr_{0.2}Mo_{0.2}Nb_{0.2}Ti_{0.2})B_2$-SiC and $(Hf_{0.2}Mo_{0.2}Ta_{0.2}Nb_{0.2}Ti_{0.2})B_2$-SiC ceramics. The effects of SiC addition on the microstructure and the corresponding mechanical properties were also discussed. SiC was found to have little effect on the microstructure refinement. In comparison with those from borothermal reduction, the HEB-SiC ceramics from boro/carbothermal reduction exhibited the finer microstructure and thus relatively high Vickers' hardness values. The ultra-hard high-entropy boride-SiC ceramic, $(Hf_{0.2}Mo_{0.2}Ta_{0.2}Nb_{0.2}Ti_{0.2})B_2$-20vol.% SiC, with a high hardness value of 29.0 GPa was obtained. Conversely, the intergranular fracture of some SiC grains was observed in the ceramics derived from borothermal reduction route, which led to the slight enhancement of fracture toughness. The current results indicated that the characteristics of the starting powders should also be considered when designing high-entropy boride-silicon carbide mateirals due to synergistic effects of processing route and secondary phase addition.

# Declarations

# Acknowledgements

This work was financially supported by State Key Laboratory for Modification of Chemical Fibers and Polymer Materials, Donghua University (No. 19ZK0113), the Pearl River S and T Nova Program of Guangzhou (No. 201710010142), Science and Technology Planning Project of Guangdong Province (No. 2017A050501033), National Natural Science Foundation of China (No. 51402055, 51602060 and U1401247), and Guangdong Innovative and Entrepreneurial Research Team Program (Grant number No. 2013G061 and 2014YT02C049).

# References

1. Fahrenholtz WG, Hilmas GE, Talmy IG, et al. Refractory diborides of zirconium and hafnium. J Am Ceram Soc. 2007;90:1347–64.

2. Liu D, Liu HH, Ning SS, et al. Chrysanthemum-like high-entropy diboride nanoflowers: A new class of high-entropy nanomaterials. J Adv Ceram. 2020. https://doi.org/10.1007/s40145-020-0373-x.
3. Liu D, Wen T, Ye B, et al. Synthesis of superfine high-entropy metal diboride powders. Scripta Mater. 2019;167:110–4.
4. Gild J, Zhang Y, Harrington T, et al. High-entropy metal diborides: a new class of high-entropy materials and a new type of ultrahigh temperature ceramics. Sci Rep. 2016;6:37946.
5. Tallarita G, Licheri R, Garroni S, et al. Novel processing route for the fabrication of bulk high-entropy metal diborides. Scripta Mater. 2019;158:100–4.
6. Gu JF, Zou J, Sun SK, et al. Dense and pure high-entropy metal diboride ceramics sintered from self-synthesized powders via boro/carbothermal reduction approach. Sci China Mater. 2019;62:1–12.
7. Zapata-Solvas E, Jayaseelan DD, Lin HT, et al. Mechanical properties of $ZrB_2$- and $HfB_2$-based ultra-high temperature ceramics fabricated by spark plasma sintering. J Eur Ceram Soc. 2013;33:1373–86.
8. Ni DW, Zhang GJ, Kan YM, et al. Hot pressed $HfB_2$ and $HfB_2$-20 vol%SiC ceramics based on $HfB_2$ powder synthesized by borothermal reduction of $HfO_2$. Int J Appl Ceram Technol. 2010;7:830–6.
9. Zhang Y, Guo WM, Jiang ZB, et al. Dense high-entropy boride ceramics with ultra-high hardness. Scripta Mater. 2019;164:135–9.
10. Zhang Y, Jiang ZB, Sun SK, et al. Microstructure and mechanical properties of high-entropy borides derived from boro/carbothermal reduction. J Eur Ceram Soc. 2019;39:3920–4.
11. Buyakova SP, Knyazeva AG, Burlachenko AG, et al. Mechanical treatment of $ZrB_2$-SiC powders and sintered ceramic composites properties. Res Develop. 2018;1:521–30.
12. Liu JX, Zhang GJ, Xu FF, et al. Densification, microstructure evolution and mechanical properties of WC doped $HfB_2$-SiC ceramics. J Eur Ceram Soc. 2015;35:2707–14.
13. Zou J, Zhang GJ, Vleugels J, et al. High temperature strength of hot pressed $ZrB_2$-20 vol% SiC ceramics based on $ZrB_2$ starting powders prepared by different carbo/boro-thermal reduction routes. J Eur Ceram Soc. 2013;33:1609–14.
14. Zhang HZ, Hedman D, Feng PZ, et al. A high-entropy B4($HfMo_2TaTi$)C and SiC ceramic Composite. Dalton Trans. 2019;48:5161–7.
15. Shen XQ, Liu JX, Li F, et al. Preparation and characterization of diboride-based high entropy $(Ti_{0.2}Zr_{0.2}Hf_{0.2}Nb_{0.2}Ta_{0.2})B_2$-SiC particulate composites. Ceram Int. 2019;45:24508–14.
16. Liu JX, Shen XQ, Wu Y, et al. Mechanical properties of hot-pressed high-entropy diboride-based ceramics. J Adv Ceram. 2020. https://doi.org/10.1007/s40145-020-0383-8.
17. Evans AG, Charles EA. Fracture toughness determinations by indentation. J Am Ceram Soc. 1976;59:371–2.

# Figures

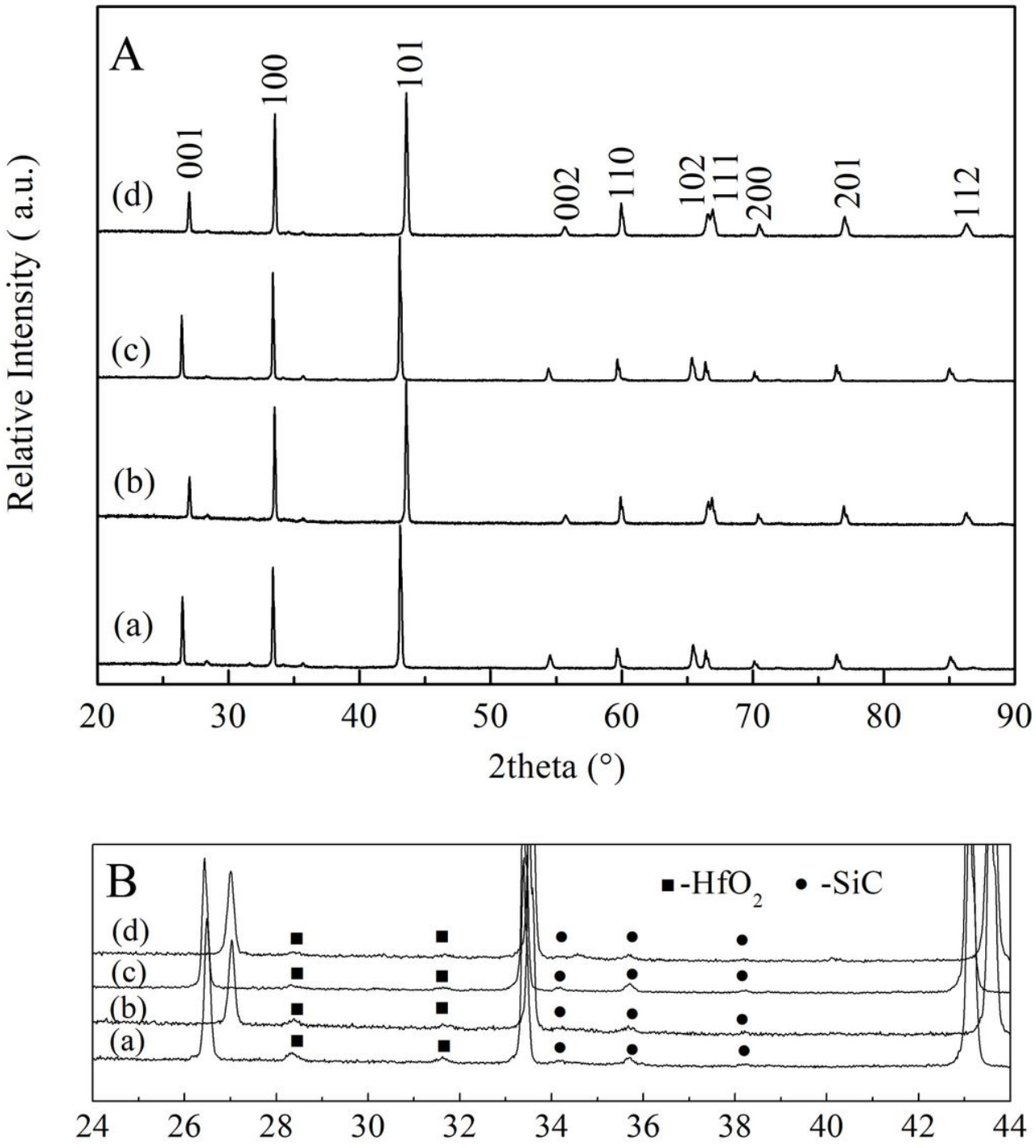


## Figure 1

A. Powder XRD patterns of the HEB-SiC ceramics after SPS at 2000oC: a: HSBR-1, b: HSBR-2, c: HSBCR-1 and d: HSBCR-2. B. Enlarged view of the PXRD patterns.

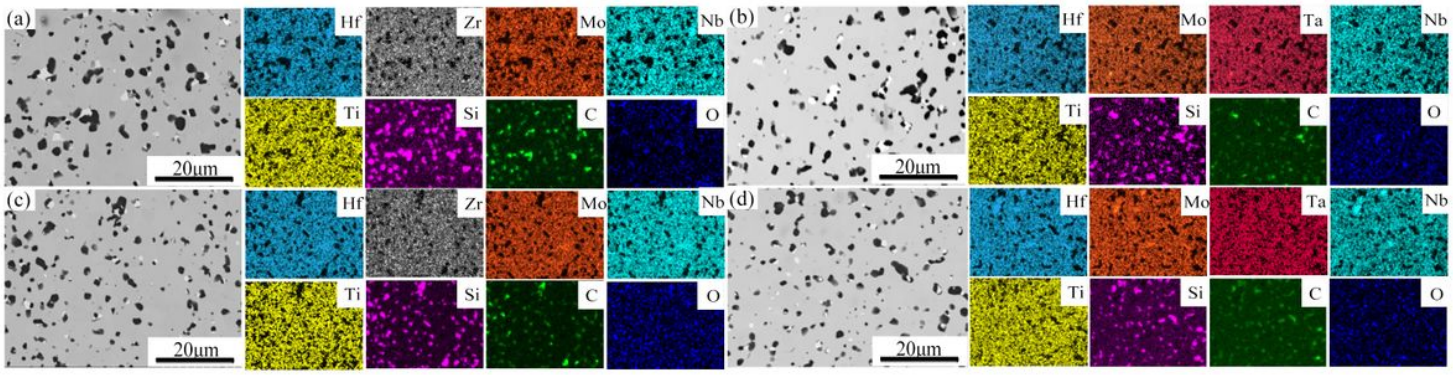


## Figure 2

EDS mapping of HEB-SiC ceramics: a: HSBR-1, b: HSBR-2, c: HSBCR-1 and d: HSBCR-2.

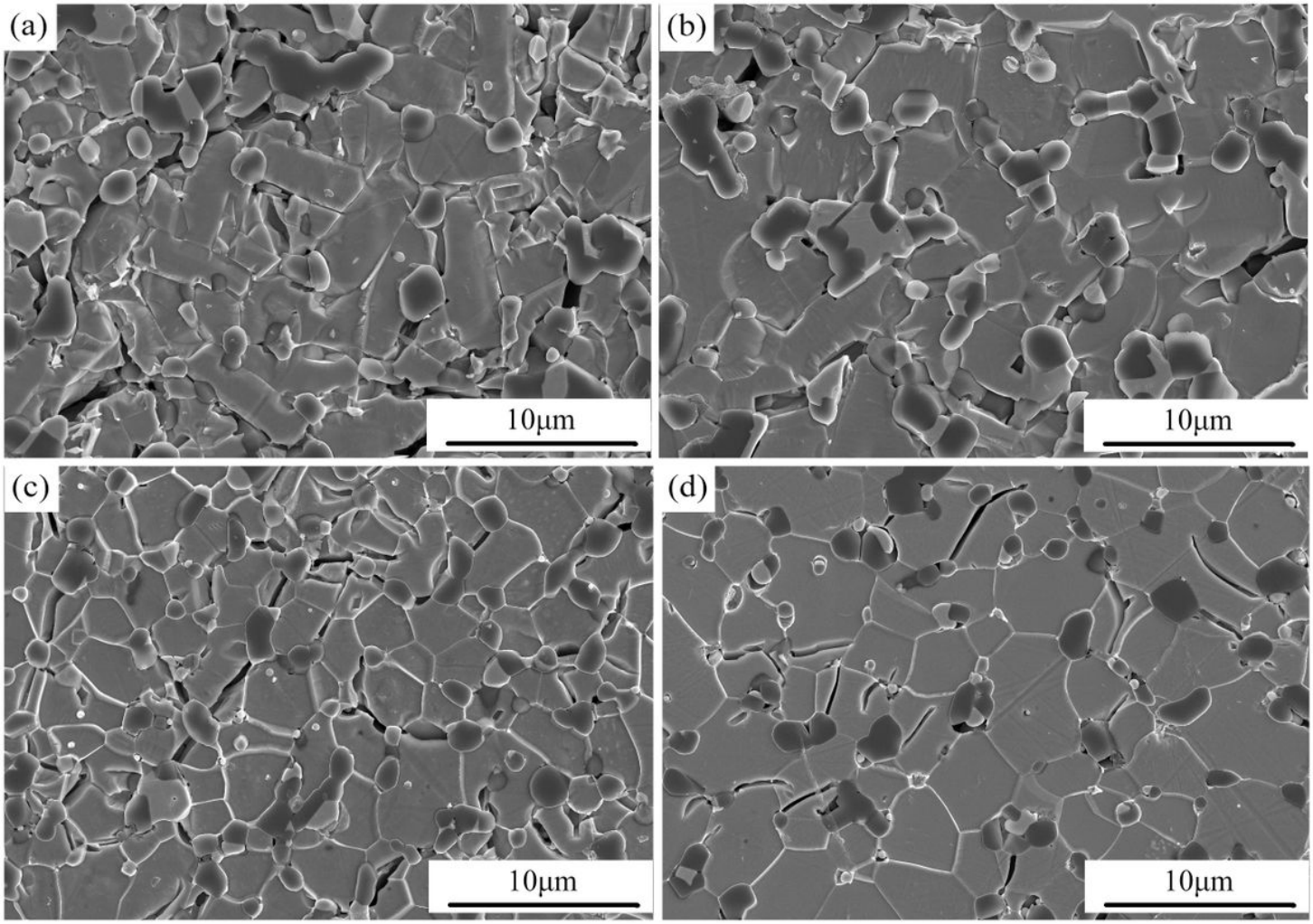


## Figure 3

SEM images of the polished surface of the HEB-SiC ceramics after etching. a: HSBR-1, b: HSBR-2, c: HSBCR-1 and d: HSBCR-2.

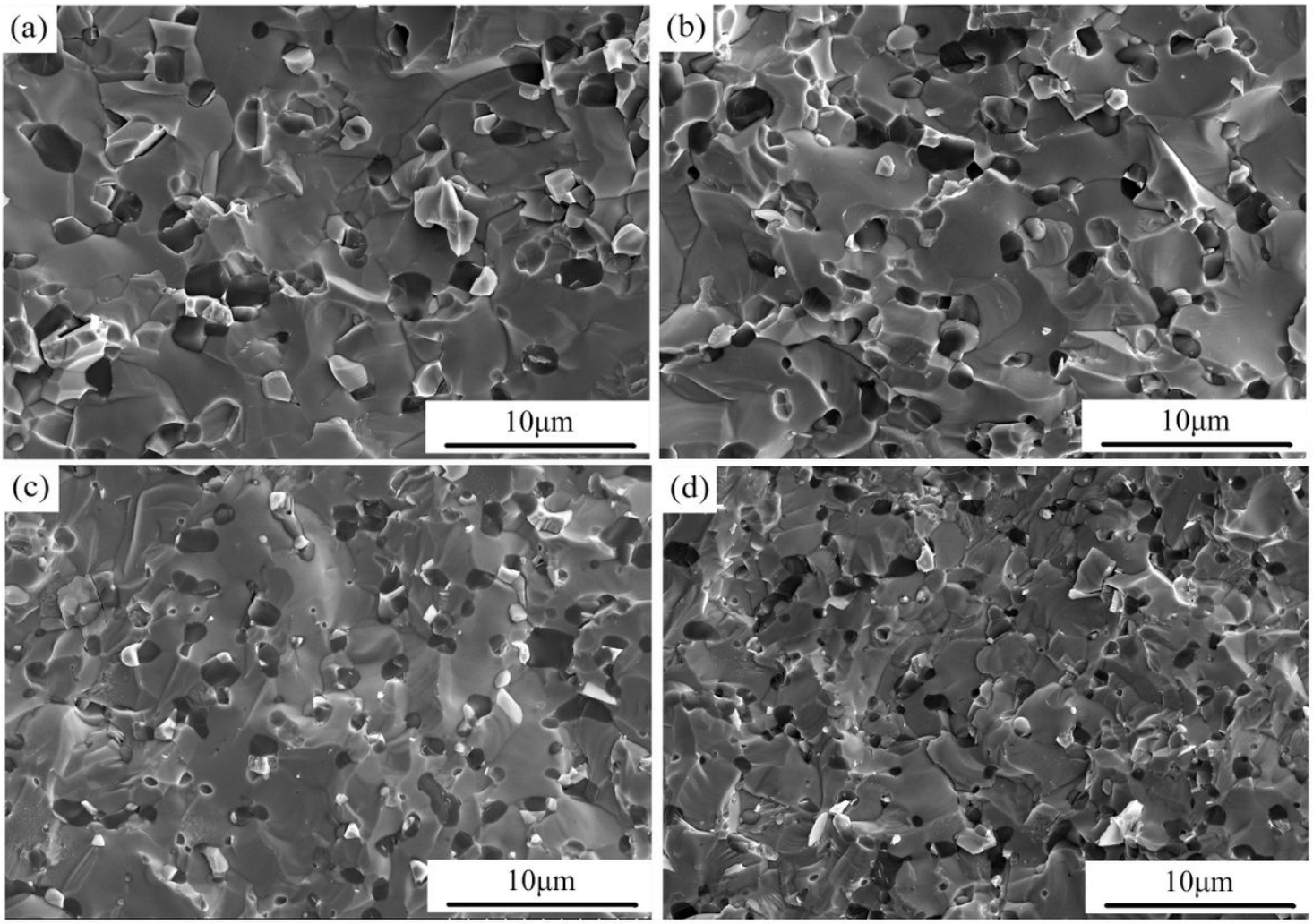


## Figure 4

SEM images of the fracture surface of the HEB-SiC ceramics. a: HSBR-1, b: HSBR-2, c: HSBCR-1 and d: HSBCR-2.